Technical Report

TR-05-05

Effect of radiation on anaerobic corrosion of iron

N R Smart and A P Rance
Serco Assurance

January 2005

Svensk Kärnbränslehantering AB
Swedish Nuclear Fuel
and Waste Management Co
Box 5864
SE-102 40 Stockholm Sweden
Tel 08-459 84 00
+46 8 459 84 00
Fax 08-661 57 19
+46 8 661 57 19

Effect of radiation on anaerobic corrosion of iron

N R Smart and A P Rance
Serco Assurance

January 2005

Executive Summary

To ensure the safe encapsulation of spent nuclear fuel elements for geological disposal, SKB of Sweden are considering using the Advanced Cold Process Canister (ACPC), which consists of an outer copper canister and a cast iron insert. A programme of work has been carried out to investigate a range of corrosion issues associated with the canister, including measurements of gas generation due to the anaerobic corrosion of ferrous materials (carbon steel and cast iron) over a range of conditions. To date, all this work has been conducted in the absence of a radiation field.

SKB asked Serco Assurance to carry out a set of experiments designed to investigate the effect of radiation on the corrosion of steel in repository environments. This report describes the experimental programme and presents the results that were obtained.

The measurements were carried out in the type of gas cell used previously, in which the change in gas pressure was measured using a liquid-filled manometer. The test cells were placed in a radiation cell and positioned so that the received radiation dose was equivalent to that expected in the repository. Control cells were used to allow for any gas generation caused by radiolytic breakdown of the construction materials and the water.

Tests were carried out at two temperatures (30°C and 50°C), two dose rates (11 Gray hr^{-1} and 300 Gray hr^{-1}), and in two different artificial groundwaters. A total of four tests were carried out, using carbon steel wires as the test material. The cells were exposed for a period of several months, after which they were dismantled and the corrosion product on one wire from each test cell was analysed using Raman spectroscopy. The report presents the results from the gas generation tests and compares the results obtained under irradiated conditions to results obtained previously in the absence of radiation.

Radiation was found to enhance the corrosion rate at both dose rates but the greatest enhancement occurred at the higher dose rate. The corrosion products were predominantly magnetite, with some indications of unidentified higher oxidation state corrosion products being formed at the higher dose rates. The main conclusions from the work are as follows:

1. The presence of gamma radiation fields increases the anaerobic corrosion rate of carbon steel in artificial groundwaters simulating those expected in the SKB repository. At 11 Gray hr^{-1} the increase only lasts for approximately 7,000 hours, but at 300 Gray hr^{-1} the enhancement is longer lasting and may be continuous.

2. The enhancement in the corrosion rate is greater in Allard water, where a 30 fold increase in corrosion rate was observed, than in bentonite-equilibrated groundwater, which had a higher ionic strength and a higher initial pH, where the radiation-induced enhancement was 10-20 times.

3. The predominant corrosion product of anaerobic corrosion of iron under irradiated conditions is magnetite, but there was some evidence of higher oxidation state oxyhydroxides under the high dose rate conditions.

4. A more detailed analysis of the radiochemical conditions in the tests is required to develop a more detailed understanding of the reasons for the increase in corrosion rate when irradiated.

Contents

Appendices

1 Introduction

To ensure the safe encapsulation of spent nuclear fuel elements for geological disposal, SKB of Sweden are considering using the Advanced Cold Process Canister (ACPC), which consists of an outer copper canister and a cast iron insert. A programme of work has been carried out to investigate a range of corrosion issues associated with the canister, including measurements of gas generation due to the anaerobic corrosion of ferrous materials (carbon steel and cast iron) over a range of conditions. To date, all this work has been conducted in the absence of a radiation field.

SKB commissioned Serco Assurance to carry out some further experiments to investigate the rate of gas generation in the presence of representative radiation fields and to analyse the composition of the corrosion product formed, to determine whether radiation has an effect on anaerobic corrosion behaviour. This work follows on from previous measurements to investigate the rate of hydrogen generation in simulated repository environments [1-8]. This report presents the results of these investigations.

2 Experimental

2.1 Test environments and materials

The measurements were carried out using gas cells of the design used in previous work. Four different environments were examined. These conditions were chosen so that comparison could be made with gas generation rate data obtained previously in the absence of radiation. The four conditions were:

Modified Allard groundwater 300 Gray hr^{-1} at 30°C

Bentonite equilibrated groundwater 300 Gray hr^{-1} at 50°C

Modified Allard groundwater 11 Gray hr^{-1} at 30°C

Bentonite equilibrated groundwater 11 Gray hr^{-1} at 50°C

The dose rates given above are based on information provided by SKB and are representative of the radiation fluxes expected to impinge on the inner and outer surfaces of the cast iron insert in the ACPC, respectively.

The solutions for the experiments were prepared from analytical grade reagents and demineralised water, according to recipes and preparation procedures provided by SKB. The composition of the artificial groundwaters is shown in Table 1.

Cold drawn carbon steel wires with the same composition as used previously were used. They were 1 mm diameter and the total exposed surface area was 0.1 m^2. The composition of the wires was as follows (wt%): C 0.21; Si 0.22; Mn 0.70; P 0.017; S 0.017; Fe bal. To minimise the amount of surface oxide present at the start of the experiments, the metal samples were pickled in inhibited hydrochloric acid, then thoroughly washed, before placing them in the test environment.

2.2 Experimental procedure

The rate of hydrogen production due to the anaerobic corrosion of steel wires in artificial groundwaters under irradiation was measured using a barometric gas cell technique of a design used previously [1-4] (Figure 1). The cell consisted of two compartments; the first compartment, containing the test specimens, was connected via a gas line to the second compartment, which was a reservoir for a low vapour pressure liquid, di-butyl phthalate (dbp). The second compartment was equipped with a glass manometer column. Any gas produced by the test pieces caused a pressure increase,

which reduced the level of dbp in the reservoir and increased the level in the manometer tube. By measuring the height of the liquid in the manometer tube and the volume of dbp displaced by expanding gas it was possible to calculate the volume of hydrogen produced by anaerobic corrosion. The results were corrected for the external atmospheric pressure. The volume of liquid in the test cells was ~150 ml.

It was thought probable that exposure of the gas cells and the water in them to radiation would result in some gas release due to radiolytic breakdown of the materials of construction and for this reason it was necessary to set up a control cell for each test environment. To minimise the gas release due to radiation, the test solutions and samples were placed in zirconia crucibles, rather than the polyethylene vessels used previously, as polyethylene was likely to suffer from radiolytic degradation. Zirconia was chosen rather than alumina because it is less susceptible to alkaline attack. The four control cells were identical to the four test cells, but did not contain any steel wires. The control cells were used to monitor the amount of gas produced by radiolytic degradation of the materials.

In the initial tests the gas taps used in the cells were made from ground glass, without any plastic components, as it was thought that these would degrade in the radiation field. However, it was found that these taps were slightly leaky to dbp, although this did not affect the validity of the gas generation readings. In later tests the normal PTFE Rotaflo taps were used, because past experience had shown that these did not leak. It was found that the PTFE tap bodies withstood the radiation field for the duration of the experiments, but some degradation of the outer non-PTFE plastic components of the valve bodies did occur, causing crumbling towards the end of the experiments. This did not affect the gas generation measurements.

The cells were prepared by posting all the cell components into a nitrogen-purged glovebox, with the exception of the precision bore manometer tube, which was too large to fit into the glovebox, but including the freshly pickled wires. This procedure was to ensure that the residual oxygen concentration in the nitrogen cover gas at the start of the experiments was minimised. The test solutions were prepared inside the glovebox. After adding the deaerated test solution to the crucible containing the test wires, the cell was assembled by joining the ground glass joints of the gas cell using two-part epoxy resin (Araldite MY753 HY951 hardener). When the epoxy resin had cured, the cells were sealed by closing the tap above the dbp reservoir and removed from the glovebox. The manometer tube was then attached and the cells were then ready to be inserted in to the radiation cell.

After assembly, each pair of cells (i.e. one test cell plus one control cell) was maintained at the required test temperature by placing them in ovens, which had openings in the top to accommodate the manometers. Lagging was placed around the exit hole for the manometers. The temperature in each of the ovens was controlled using a Eurotherm temperature controller and type K thermocouple. The required γ-radiation dose rates were achieved by placing the ovens at appropriate distances from the cobalt-60 source in Centronic Raditec's gamma irradiation facility at Harwell, Oxfordshire, U.K. The layout of the test cells in the radiation facility is shown in Figure 2 (this figure shows the two tests with bentonite-equilibrated water). The dose rates were measured directly using a Farmer dose meter and ion chamber, which were calibrated to national standards.

Gas production measurements were made at appropriate intervals to accommodate the expected initial high rate and the subsequent rate reduction. The procedures for measuring the amount of gas generated and calculating the corresponding corrosion rates are given in Appendix 1 and 2. From time to time it was necessary to refill the dbp reservoir as the level was reduced by the evolution of gas. The procedure for doing this is given in Appendix 3. Due to essential refurbishment work on the radiation cell it was necessary to remove some of the gas cells from the radiation test facility cell for a few weeks during the course of the experiments.

2.3 Analysis of samples

At the end of the experiments the cells were dismantled and the pH values of the solutions were measured. Photographs were taken to show the condition of the test specimens at the end of the

exposure period. One wire from each cell was analysed by Raman spectroscopy to determine the composition of the corrosion product. The cells were dismantled in a nitrogen-purged glove box and single wires, which were still wetted by the test solution, were sealed in capillary tubes to ensure that they were not exposed to air. The capillary tubes were sealed with a blob of Araldite, which was allowed to harden. The tubes were then removed from the glovebox and the glass was sealed by rapidly fusing it in a gas flame at a point well away from the sample so that the latter was not heated significantly. The sample was then transferred to the Raman spectrometer for analysis.

A Renishaw Laser Raman Microprobe was used to analyse the surface of the corroded wires through the glass walls of the capillary tubes. The exciting laser wavelength of 688 nm was obtained using a red HeNe laser, capable of delivering up to 100 mW total power, measured at the output from the laser. The detector was a peltier-cooled CCD array. The laser was coupled to the sample via a 180^{o} backscattered arrangement using a Leitz optical microscope with high numerical aperture objective lenses (x20 and x50 magnification). The Rayleigh scattered light was removed via a notch filter and the Raman scattered light dispersed via holographic diffraction gratings. The spectrometer was capable of recording over a wide wavenumbers shift range, but spectra were recorded over a limited range of ca. 200 to 800 cm^{-1}, which covered the main bands expected from iron corrosion products.

3 Results

3.1 Measurements in Allard groundwater

The results of the gas generation experiments in Allard water at two radiation levels at 30 ºC are shown in Figure 4 and Figure 5. The corrosion rate data are based on the assumption that the final corrosion product was magnetite (Fe_3O_4), formed by the overall reaction:

$$3Fe + 4H_2O \rightarrow Fe_3O_4 + 4H_2\uparrow \quad (1)$$

For comparison, the data obtained for carbon steel in unirradiated Allard water at 30 ºC are also given in Figure 5 and Figure 6; the data for unirradiated conditions were taken from earlier studies [3,5,7]. The Allard water used for the unirradiated tests had a slightly different composition to that used for the irradiated tests, as shown in Table 3.

3.2 Measurements in bentonite-equilibrated groundwater

The results of the gas generation experiments in bentonite-equilibrated groundwater at two radiation levels at 50 ºC are shown in Figure 6 and Figure 8. For comparison purposes, the data for carbon steel in unirradiated bentonite-equilibrated groundwater at 50 ºC [4] are also shown.

3.3 Analysis of corrosion product

The condition of the specimens removed from the test cells can be seen in Figure 9 and Figure 10. The samples tested at the low dose rate were black and the solution was clear, whereas the solution tested at the high dose rate had a milky appearance and the corrosion product had a slight brown tinge to it. It was also found that there was a layer of dark brown sludge at the bottom of the test cell.

Multiple Raman spectra were recorded from each of the samples and a representative spectrum from each is shown in Figure 11 to Figure 13. All three wire samples displayed a strong Raman band at ca. 660 cm^{-1} and this is indicative of magnetite. For comparison, the reference spectrum of magnetite is overlaid on these spectra [9]. Reference spectra of three commonly encountered corrosion products of iron, namely magnetite, haematite and goethite, are shown in Figure 14 to Figure 16. Other phases of oxidised iron, in particular the oxyhydroxides, may also have been present, although no definitive attribution could be made from the data. Table 1 lists the peak positions of three different FeOOH phases [10]. There were no indications of iron carbonate, or green rusts, a series of Fe(II)-Fe(III) compounds, for which a characteristic peak at 430 cm^{-1} would be expected [11].

The pH of the test solution in the cells containing the wires was measured after dismantling and the results are shown in Table 3.

4 Discussion

Tests have been carried out to measure the anaerobic corrosion rates of steel and the corresponding hydrogen generation rates under radiation levels simulating those on the inner and outer surfaces of the cast iron insert, using two simulated groundwaters, two test temperatures and two radiation levels. Some gas generation was measured from the dummy cells (Figure 3) but it was considerably less than that measured for the test cells containing wires. The gas generation rate in the dummy cells appeared to be highest at the highest radiation dose, presumably due to radiolytic breakdown of the cell components or contents.

At 30 ºC and a dose rate of 11 Gray hr^{-1}, the corrosion rate in Allard water was higher than in unirradiated conditions (Figure 4) by a factor of about 6 initially, but after 7000 hours the corrosion rate was similar to the corrosion rate for unirradiated conditions, suggesting that once the corrosion product film had become fully developed the effect of radiation was negligible. At the same temperature, but at a dose rate of 300 Gray hr^{-1} (Figure 5), the initial corrosion rate was also higher than in unirradiated conditions, but the increase in corrosion rate was maintained over the entire test period. This test was interrupted, because it was necessary to remove the cell from the radiation cell during the course of the experiment for essential maintenance, but when the cell was re-exposed to the radiation source, there was an increase in gas generation. This supports the view that the presence of radiation increased the corrosion rate. The final reading on the test cells gave a corrosion rate value of ~3 $\mu m\ year^{-1}$, compared to <0.1 $\mu m\ year^{-1}$ without radiation.

At 50 ºC and 11 Gray hr^{-1}, both tests in bentonite-equilibrated groundwater gave a higher corrosion rate initially compared to the results obtained previously under unirradiated conditions (Figure 6). However after ~2,000 hours, the corrosion rate was very similar to that measured in the absence of radiation (Figure 7), and after ~4,000 hours the corrosion rate for both irradiated and unirradiated conditions was ~0.05-0.2 $\mu m\ year^{-1}$. At the higher dose rate (i.e. 300 Gray hr^{-1}), the corrosion rate remained higher throughout the test (Figure 8), and after 5000 hours the corrosion rate was ~0.8 $\mu m\ year^{-1}$ compared to 0.05 $\mu m\ year^{-1}$ without radiation. Approximately 25% of this apparent increase in corrosion rate at 5,000 hours was probably attributable to gas production from other materials within the cell apart from the steel, as shown by the dummy cell results (Figure 3). Nevertheless there appears to be a real increase in corrosion rate as a result of the high radiation dose.

For comparison, Marsh and Taylor [12] carried out corrosion experiments on 0.2% carbon forged steel in argon-purged synthetic groundwater (pH 9.4), with and without radiation. The ionic strength and pH of the artificial groundwater used in their work were similar to the Allard water used in the present tests (Table 3). On the basis of weight loss measurements, Marsh et al found that the integrated corrosion rate after 5,000 hours in unirradiated conditions was ~0.1 $\mu m\ year^{-1}$, with no localised attack. In the same environment with a radiation dose of 1,000 Gray hr^{-1}, the corrosion rate was constant at ~3 $\mu m\ year^{-1}$, for test periods of up to 5236 hours, with no localised attack developing. These corrosion rates are similar to those measured in the current work in the Allard water, as shown in Figure 5. No localised attack was observed in the current tests either. The fact that similar corrosion rates have been observed on the basis of weight loss and hydrogen generation measurements suggests that the increased volume of hydrogen produced is a result of corrosion, rather than radiolysis processes in the test cell.

Other workers have reported that the corrosion rates of iron-based alloys under irradiated conditions are generally 2 to 3 times higher than those obtained on similar materials under non-irradiated conditions at 150 ^{o}C [13].

The main corrosion product detected by Raman spectroscopy was magnetite, although there is a possibility that there was also a small amount of FeOOH present. Comparison with Raman spectra

acquired for wires that had been corroded in the absence of radiation [14] shows that radiation may led to the formation of some additional iron oxy-hydroxide species, which showed up as additional peaks in the Raman spectra at lower wavenumbers than the magnetite peak, but it has not been possible to conclusively attribute these peaks to specific species. It was observed that the corrosion product formed under a high dose rate was a different colour to the specimens produced at 0 Gray hr^{-1} or 11 Gray hr^{-1} – it had a brownish tinge to it, rather than being completely black. There also appeared to be more corrosion product produced, which collected as a sludge at the bottom of the cell. These results suggest that the presence of radiolysis species in the solution leads to the formation of different higher oxidation state iron corrosion products, as well as magnetite, but their exact composition has not been characterised.

When water radiolysis occurs, hydrogen, hydrogen peroxide, hydroxyl radicals, aqueous electrons, oxygen and a number of other reactive species may be formed [15]. However the concentration of the various species will depend on a number of factors [16,17] including the composition of the solution under irradiation [18], the dose rate and the concentration of hydrogen produced by the corrosion reaction. To obtain a fuller understanding, more detailed radiochemical modelling of the conditions in the present tests would be required.

5 Conclusions

The main conclusions from this work are as follows:

1. The presence of gamma radiation fields increases the anaerobic corrosion rate of carbon steel in artificial groundwaters simulating those expected in the SKB repository. At 11 Gray hr^{-1} the increase only lasts for approximately 7,000 hours, but at 300 Gray hr^{-1} the enhancement is longer lasting and may be continuous.

2. The enhancement in the corrosion rate is greater in Allard water, where a 30 fold increase in corrosion rate was observed, than in bentonite-equilibrated groundwater, which had a higher ionic strength and a higher initial pH, where the radiation-induced enhancement was 10-20 times.

3. The predominant corrosion product of anaerobic corrosion of iron under irradiated conditions is magnetite, but there was some evidence of higher oxidation state oxyhydroxides under the high dose rate conditions.

4. A more detailed analysis of the radiochemical conditions in the tests is required to develop an improved understanding of the reasons for the increase in corrosion rate under irradiation.

6 References

1 D.J. Blackwood, A.R. Hoch, C.C. Naish, A.P. Rance and S.M. Sharland, *Research on Corrosion Aspects of the Advanced Cold Process Canister*, AEA-D&W-0684, SKB Technical Report 94-12, 1994.

2 D.J. Blackwood, C.C. Naish and A.P. Rance, *Further Research on Corrosion Aspects of the Advanced Cold Process Canister*, AEA-ESD-0052, SKB-PR-95-05, 1994.

3. D.J. Blackwood, C.C. Naish, N. Platts, K.J. Taylor & M.I. Thomas, *The Anaerobic Corrosion of Carbon Steel in Granitic Groundwaters*, AEA Technology Report, AEA-InTec-1414, 1995.

4 N.R Smart, A.P. Rance and D.J. Blackwood, *Corrosion Aspects of the Copper-steel/iron Process Canister: Consequences of Changing the Material for the Inner Container from Carbon Steel to Cast Iron*, SKB 97-04, 1997.

5 N.R. Smart, D.J. Blackwood and L. Werme, *The Anaerobic Corrosion of Carbon Steel and Cast Iron in Artificial Groundwaters*, SKB Report TR-01-22, 2001.

6 N.R. Smart, D.J. Blackwood and L. Werme, *Anaerobic Corrosion of Carbon Steel and Cast Iron in Artificial Groundwaters: Part 1–Electrochemical Aspects*, Corrosion **58**(7), 547, 2002.

7 N.R. Smart, D.J. Blackwood and L. Werme, *Anaerobic Corrosion of Carbon Steel and Cast Iron in Artificial Groundwaters: Part 2-Gas Generation*, *Corrosion* **58**(8), 627, 2002.

8 N.R. Smart, A.P. Rance and L.O. Werme, *Anaerobic Corrosion of Steel in Bentonite*, in Scientific Basis for Nuclear Waste Management XXVII, Materials Research Society Symposium Proceedings Volume 807, V.M. Oversby and L.O. Werme (eds.), p. 441-446, 2004.

9 From California Institute of Technology Mineral Database.

10 D.L.A. de Faria, S. Venâncio Silva and M.T. Oliveira, *Raman Microspectroscopy of Some Iron Oxides and Oxyhydroxides*, J Raman Spectroscopy **28**, 873-878, 1997.

11 Ph. Refait, J-B Memet, C. Bon, R. Sabot and J.M.R. Génin, *Formation of the Fe(II)-Fe(III) Hydroxysulphate Green Rust During Marine Corrosion of Steel*, Corrosion Science **45**, 833-845, 2003.

12 G.P. Marsh and K.J. Taylor, *An Assessment of Carbon Steel Containers for Radioactive Waste Disposal*, Corrosion Science **28**, 289-320, 1988.

13 J.L. Nelson, R.E. Westerman and F.S. Gerber, *Irradiation-Corrosion Evaluation of Metals for Nuclear Waste Package Applications in Grande Ronde Basalt Groundwater* in Scientific Basis for Nuclear Waste Management X, , Materials Research Society Symposium Proceedings Volume 26, G.L. McVay (ed.), p. 121-128, 1984.

14 A.P. Rance, R. Peat and N.R. Smart, *Analysis of SKB Electrochemistry Cells*, SA/RJCB/62036/R01, and SKB report TR-04-01, 2003.

15 Z. Cai, X. Li, Y. Katsumura and O. Urabe, *Radiolysis of Bicarbonate and Carbonate Aqueous Solutions: Product Analysis and Simulation of Radiolytic Processes*, Nuclear Technology **136**, 231, 2001.

16 H. Christensen and S. Sunder, *An Evaluation of Water Layer Thickness Effective in the Oxidation of UO_2 Fuel Due to Radiolysis of Water*, Journal of Nuclear Materials **238**, 70-77, 1996.

17 G.V. Buxton, C.L. Greenstock, W.P. Hellman and A.B. Ross, *Critical Review of Rate Constants for Reactions of Hydrated Electrons, Hydrogen Atoms and Hydroxyl Radicals in Aqueous Solutions*, J. Phys. Chem. Reference Data **17**, 513 – 886, 1988.

18 S. Sunder and H. Christensen, *Gamma Radiolysis of Water Solutions Relevant to the Nuclear Waste Management Program*, Nuclear Technology **104**, 403, 1993.

Ion	Bentonite-equilibrated water		Allard water for radiation experiments‡		Allard water for previous measurements [7]	
	mM	ppm	mM	ppm	mM	ppm
Na^+	560	12880	2.3	52.5	2.84	65.3
Ca^{2+}			0.13	5.1	0.45	18.0
Mg^{2+}			0.03	0.7	0.18	4.4
K^+			0.10	3.9	0.10	3.9
Cl^-	540	19170	1.4	48.8	1.96	69.5
HCO_3^-			1.1	65.0		
CO_3^{2-}	10	600			2.00†	120.0
SO_4^{2-}			0.10	9.6	0.1	9.6
SiO_2			0.03	1.7	0.21	12.6
pH*	10.4		8.8		8.1	

* pH was adjusted by addition of NaOH or HCl as necessary.
† total carbonate
‡ prepared in nitrogen-purged glovebox

Table 1. Composition of artificial groundwaters used for corrosion experiments

Mineral	Formula	Peak positions
Goethite	α-FeOOH	243, 299, 385 (main), 479, 550
Lepidocrocite	γ-FeOOH	245 (main), 373, 522 (minor)
-	δ-FeOOH	400 (very broad), 680 (broad)

Table 2. Raman Peak Positions of FeOOH Phases

Cell number	Environment	pH at end of test
5	Allard groundwater 300 Gray hr^{-1} @ 30°C	Not dismantled
2	Bentonite equilibrated groundwater 300 Gray hr^{-1} @ 50°C	9.07
7	Allard groundwater 11 Gray hr^{-1} @ 30°C	9.30
1a	Bentonite equilibrated groundwater 11 Gray hr^{-1} @ 50°C	8.97

Table 3. pH of test solutions containing wires at end of gas measurement experiments

Dose (kGy)	e^-_{aq}	H	OH	H_2O_2
1	0.27	0.06	0.28	0.07
5	1.4	0.3	1.4	0.4
10	2.7	0.6	2.8	0.7

Table 4. Estimated concentrations (mmol/l) of transient reactive species in pure water [Error! Bookmark not defined.**].**

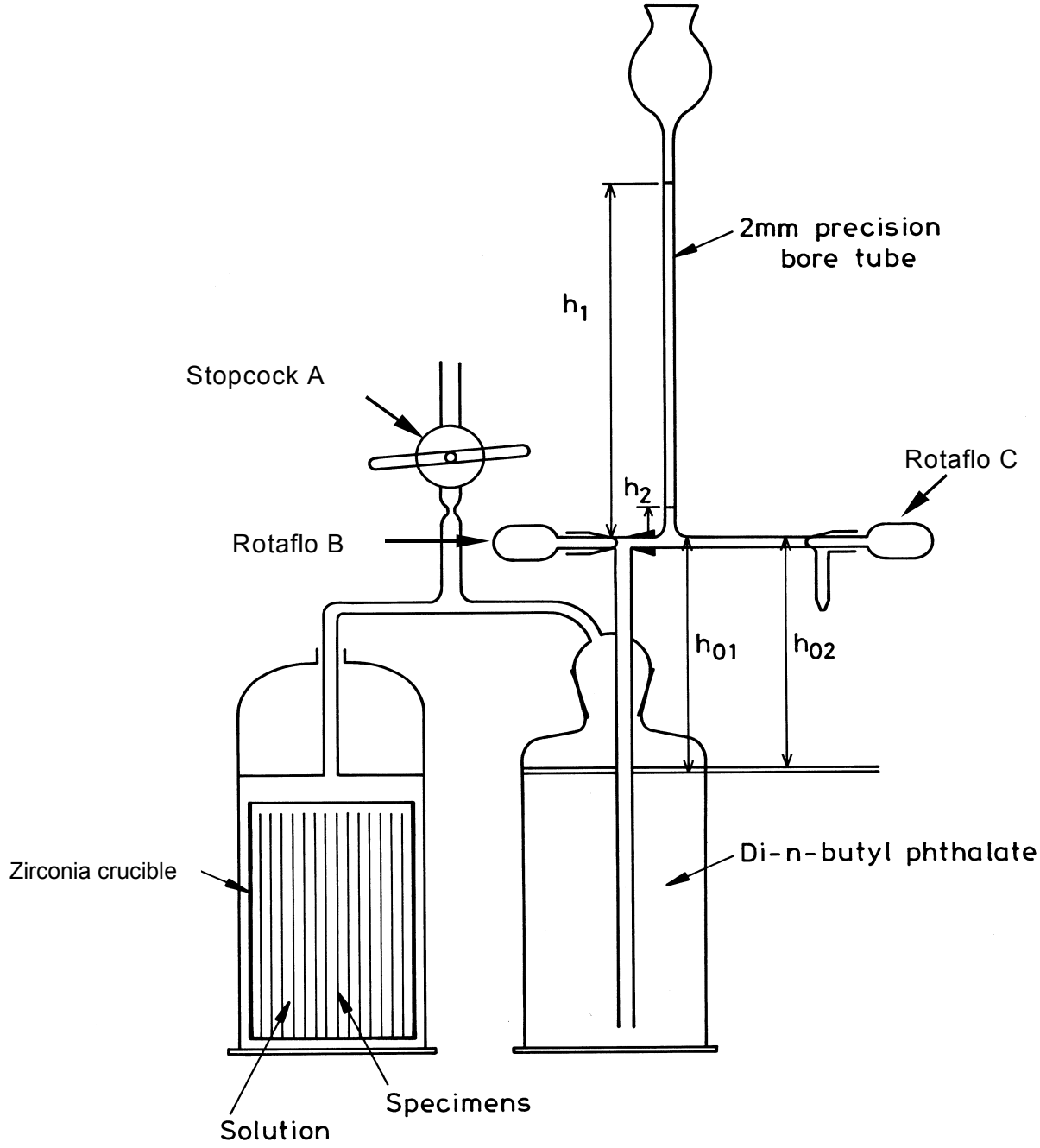

Figure 1. Diagram of gas cell used to measure hydrogen production due to anaerobic corrosion of carbon steel under irradiated conditions.

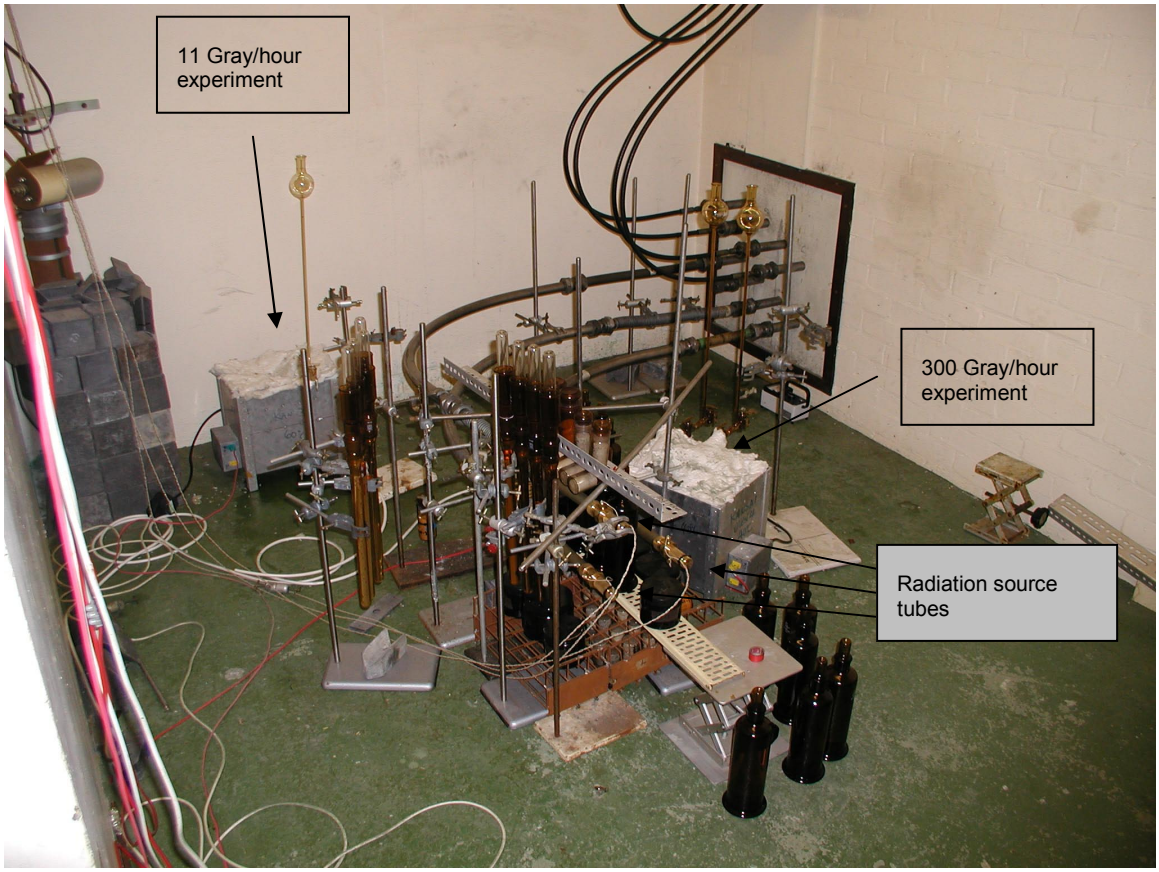

Figure 2. Layout of corrosion experiments in radiation cell.

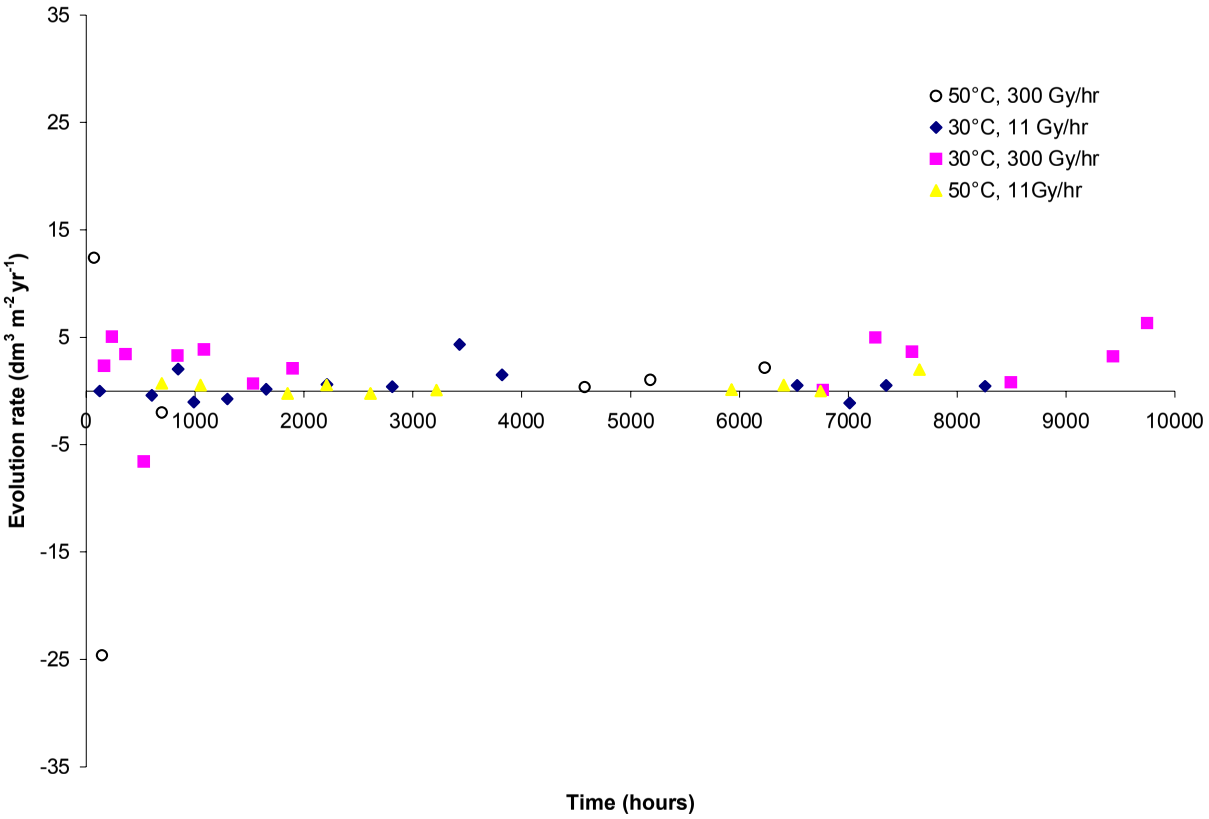

Figure 3. Gas evolution rate from dummy cells.

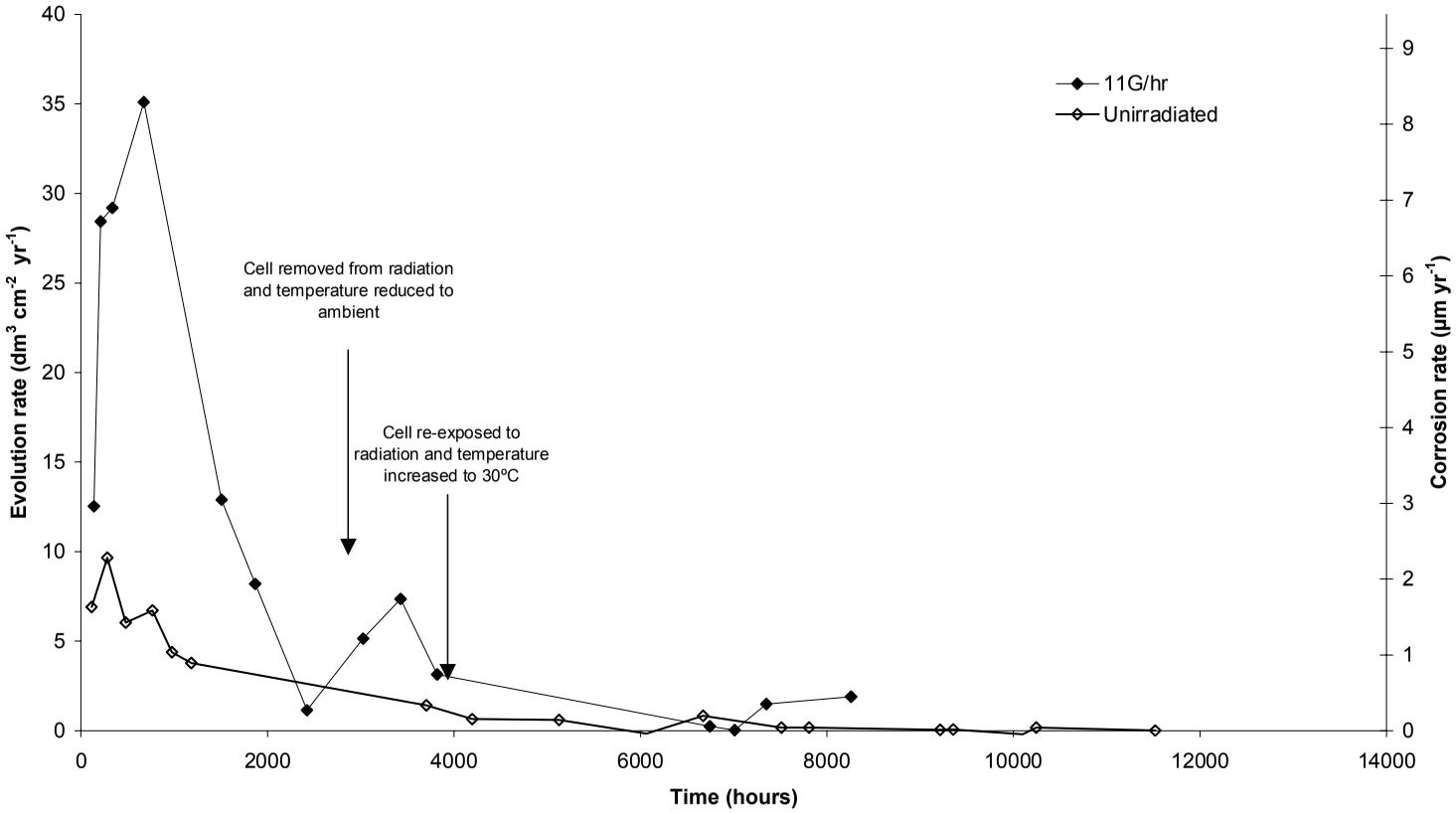

Figure 4. Hydrogen evolution rates and corrosion rates for carbon steel in anoxic Allard water at 30ºC and 0 Gray hour^{-1} and 11 Gray hour^{-1} (see Table 1 for composition of Allard waters).

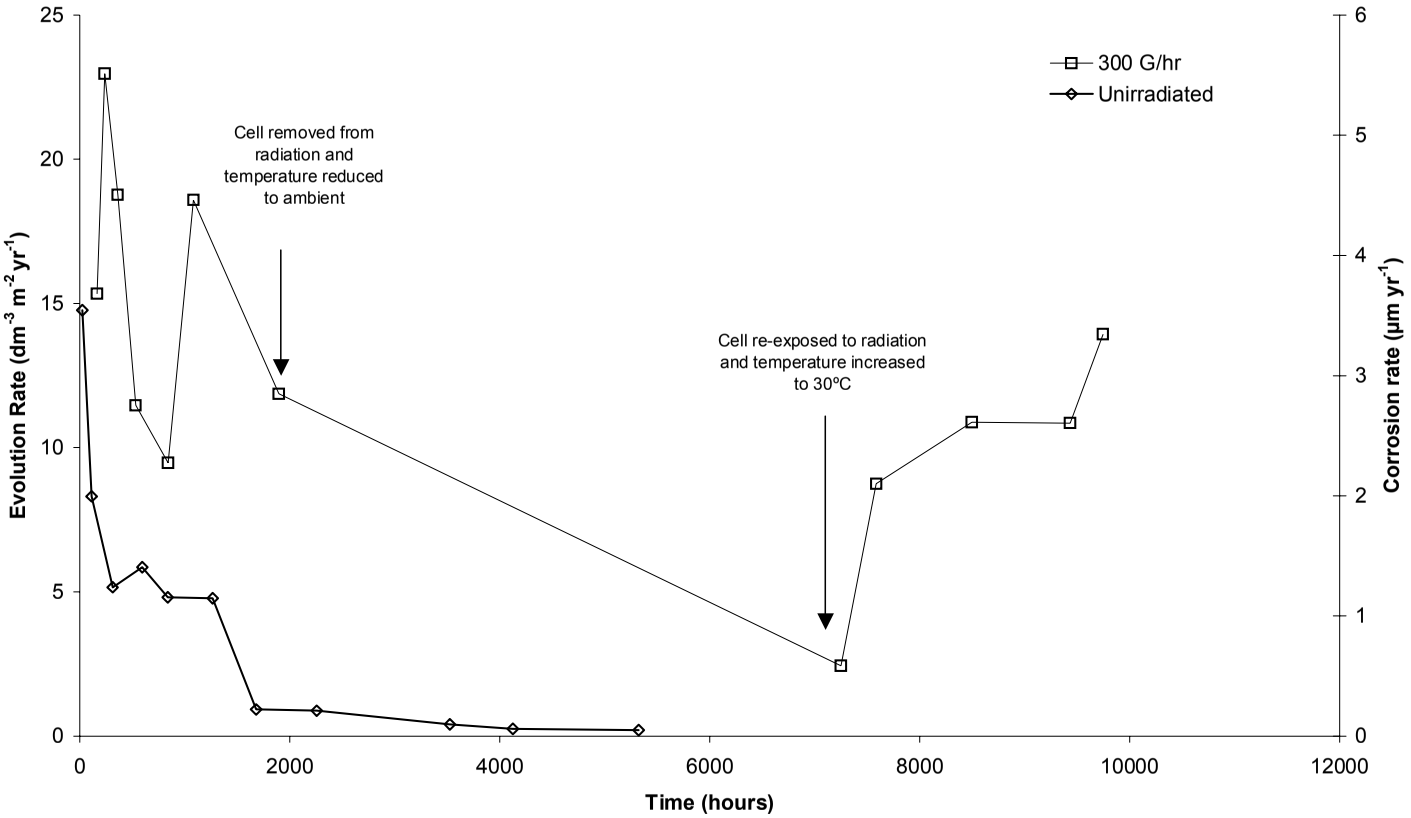

Figure 5. Hydrogen evolution rates and corrosion rates for carbon steel in anoxic Allard water at 30ºC and 0 Gray hour^{-1} and 300 Gray hour^{-1} (see Table 1 for composition of Allard waters).

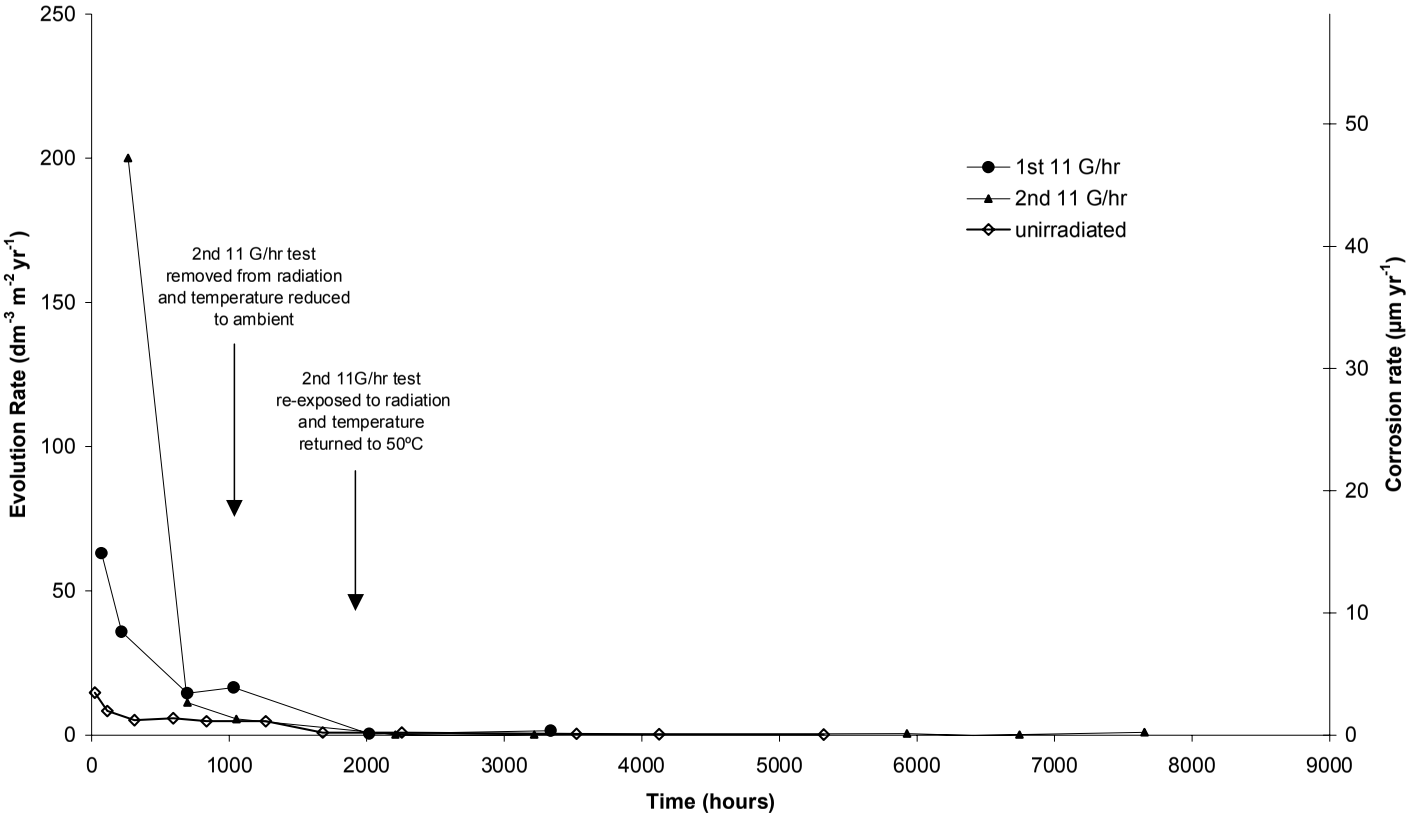

Figure 6. Hydrogen evolution rates and corrosion rates for carbon steel in anoxic bentonite-equilibrated groundwater at 50ºC at 0 Gray hour^{-1} and 11 Gray hour^{-1}.

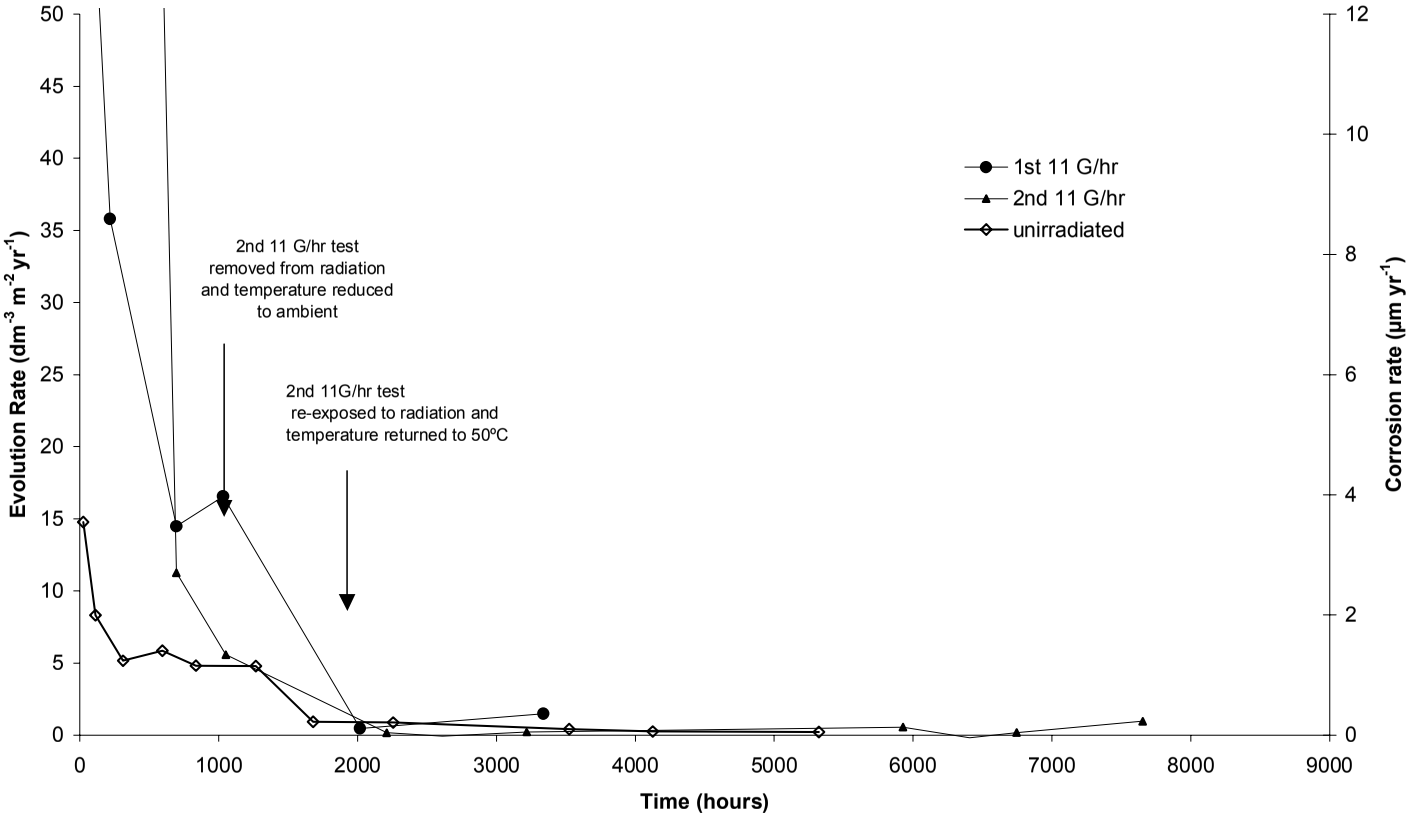

Figure 7. Hydrogen evolution rates and corrosion rates for carbon steel in anoxic bentonite-equilibrated groundwater at 50ºC at 0 Gray hour^{-1} and 11 Gray hour^{-1} – expanded scale.

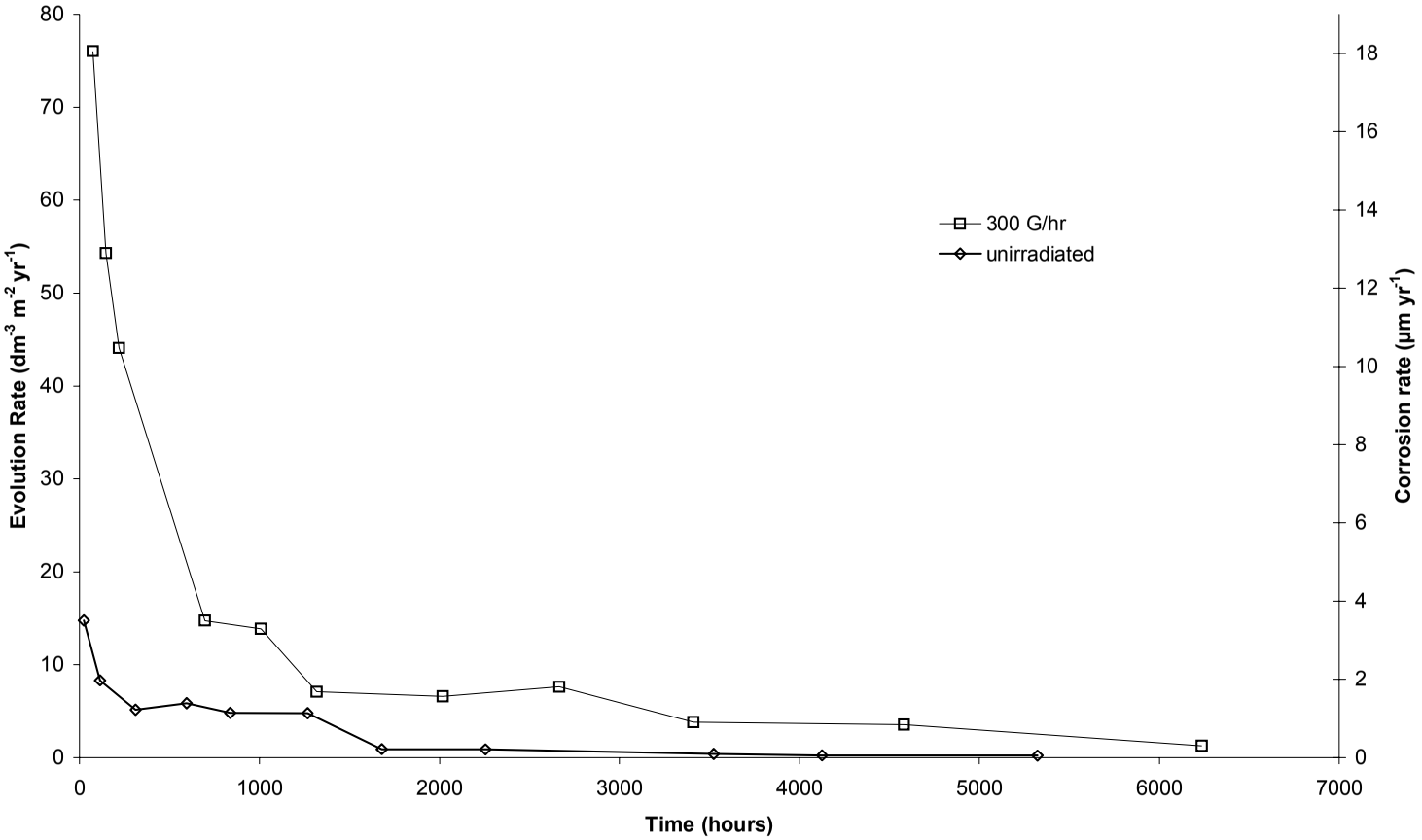

Figure 8. Hydrogen evolution rates and corrosion rates for carbon steel in anoxic bentonite-equilibrated groundwater at 50ºC at 0 Gray hour^{-1} and 300 Gray hour^{-1}.

Figure 9. Condition of specimens on completion of corrosion experiments: LHS: Cell 7 Allard groundwater, 11 Gray hr^{-1} at 30°C, RHS: Cell 1, Bentonite-equilibrated groundwater, 11 Gray hr^{-1} at 50°C.

Figure 10. Condition of specimens on completion of corrosion experiments: Cell 2, Bentonite-equilibrated groundwater 300 Gray hr^{-1} at 50°C.

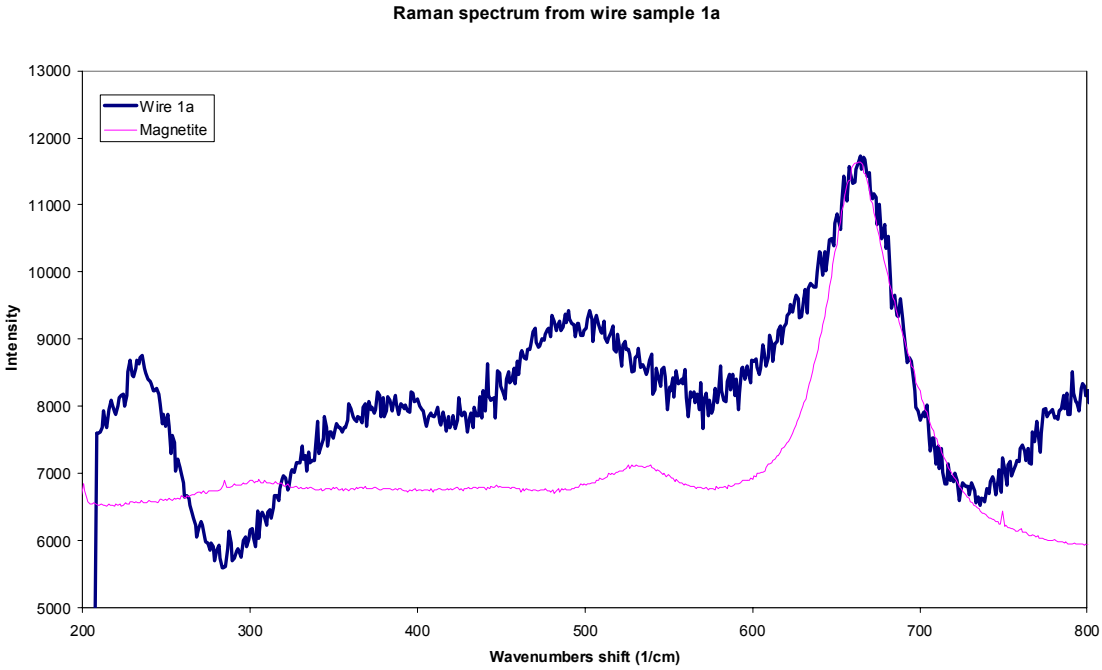

Figure 11. Raman spectrum for corrosion product formed on carbon steel wire in anoxic bentonite-equilibrated groundwater at 50ºC and 11 Gray hour^{-1}.

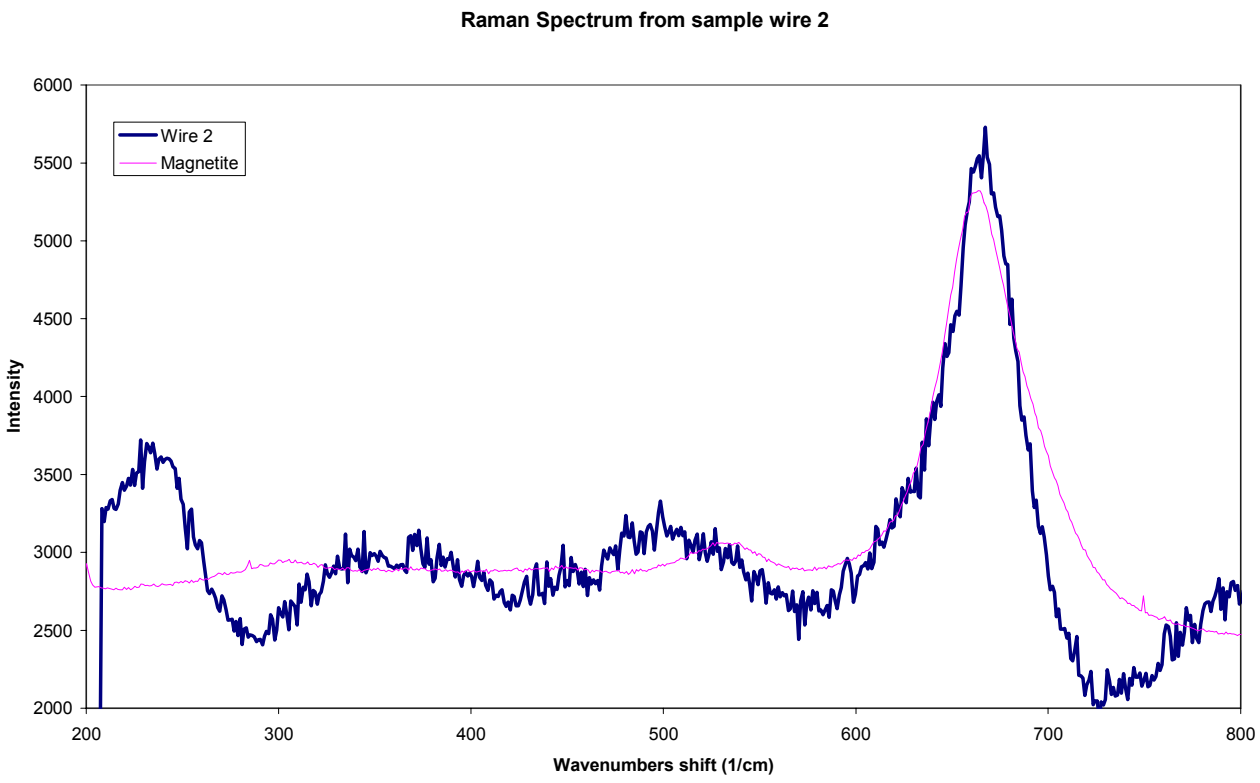

Figure 12. Raman spectrum for corrosion product formed on carbon steel wire in anoxic bentonite-equilibrated groundwater at 50ºC and 300 Gray hour^{-1}.

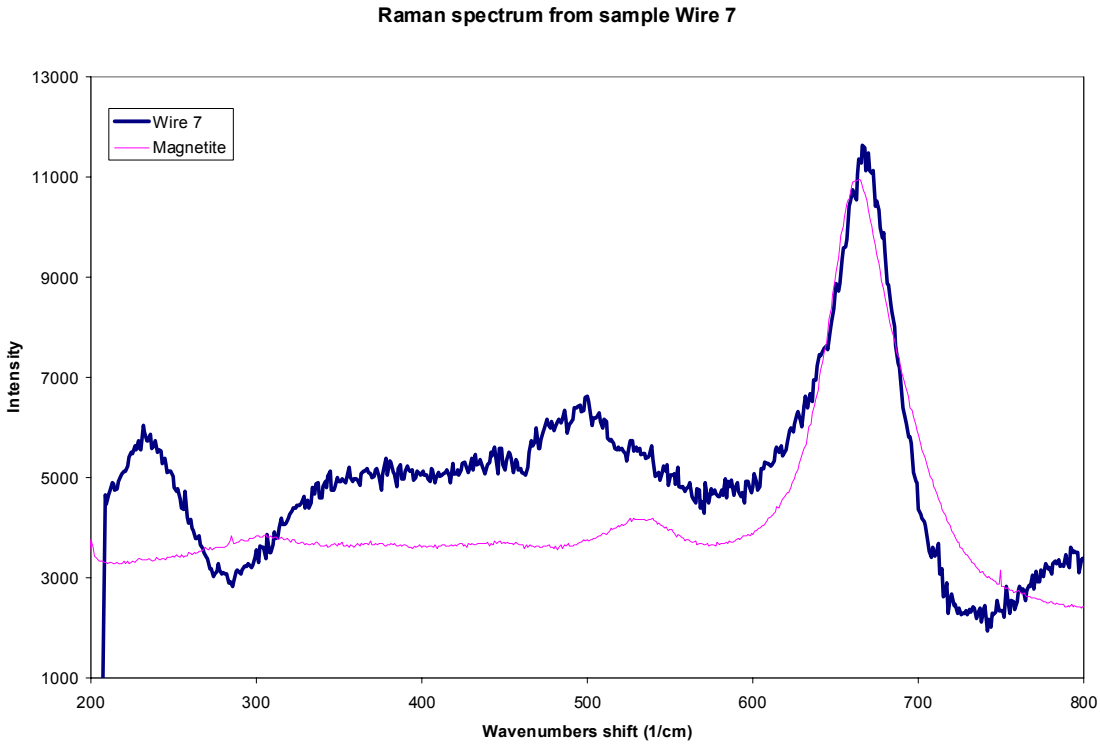

Figure 13. Raman spectrum for corrosion product formed on carbon steel wire in anoxic Allard groundwater at 30ºC and 11 Gray hour^{-1}.

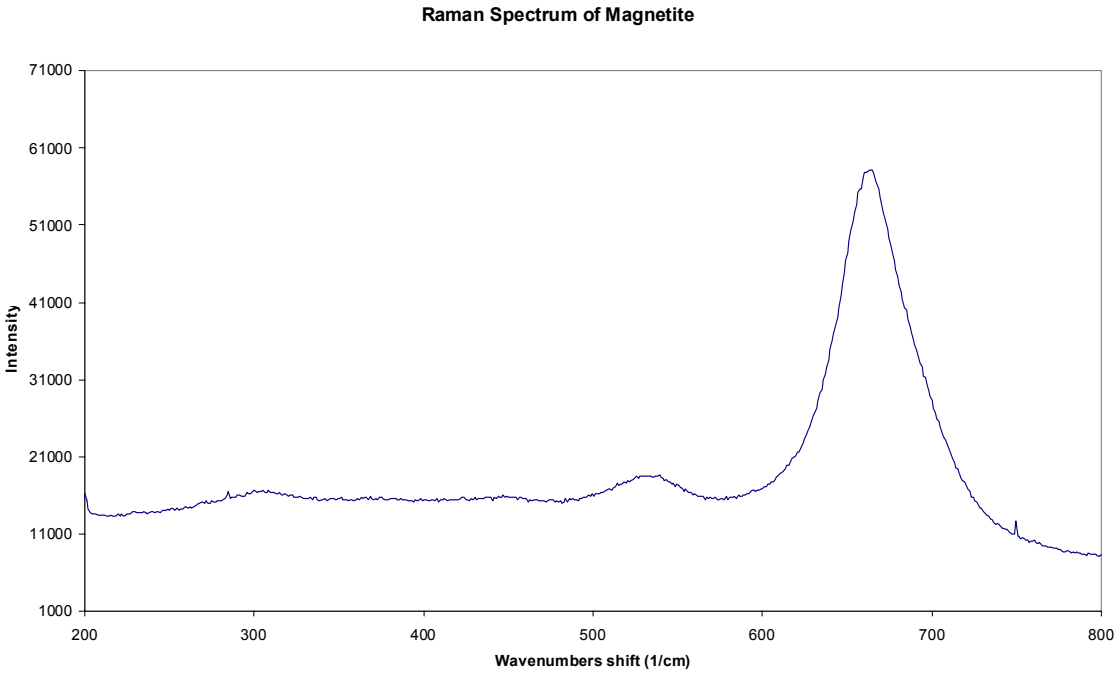

Figure 14. Raman spectra for magnetite.

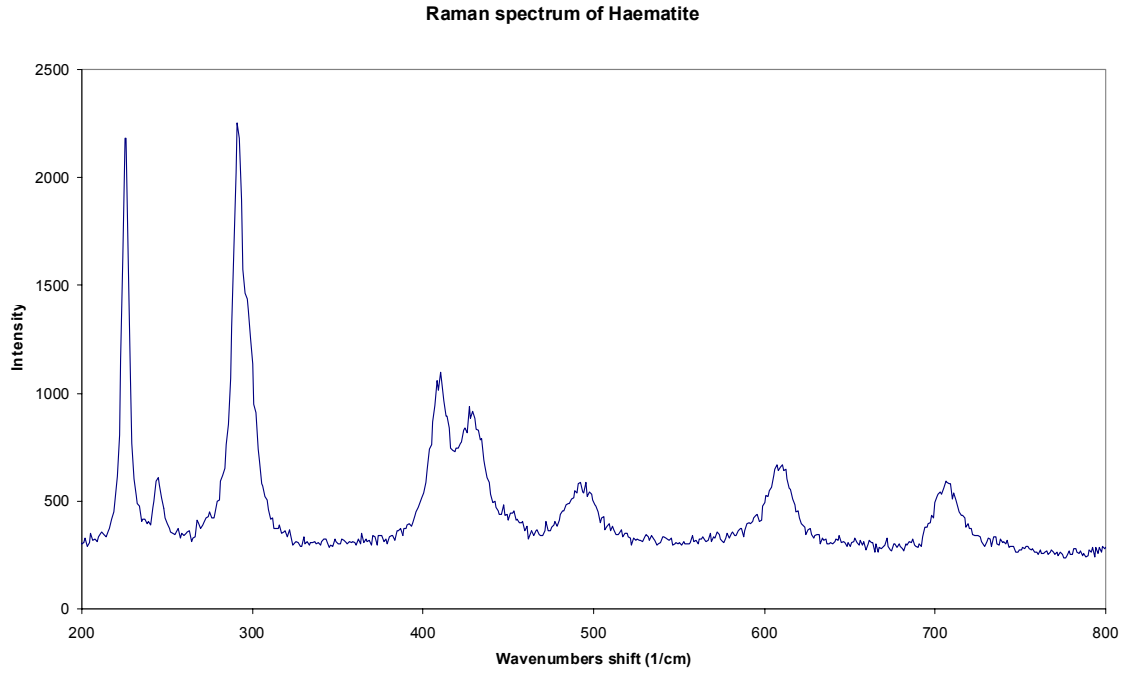

Figure 15. Raman spectra for haematite.

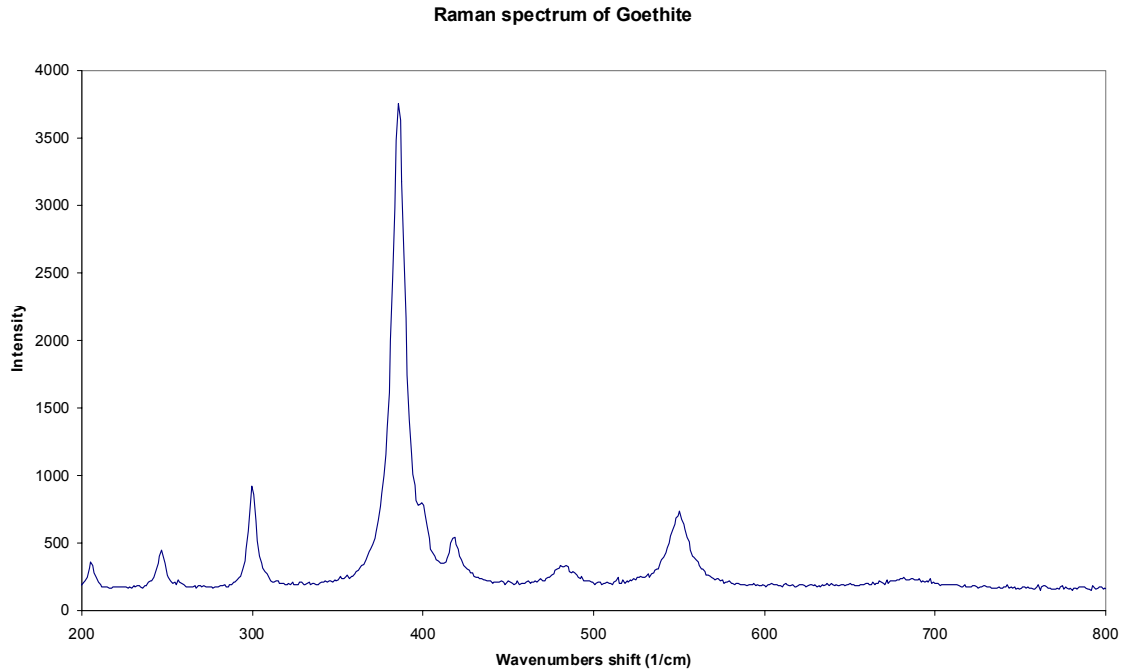

Figure 16. Raman spectra for Goethite.

Appendices

CONTENTS

Appendix 1
Gas Measurement and Calculations for DBP Cells

The aim of the measurement is to obtain a value for the volume and pressure of hydrogen inside the gas cell. This is achieved by introducing a change in volume of the gas in the cell, by draining off some of the liquid in the gas displacement column, and calculating the resulting changes in volume and pressure. By applying the ideal gas laws it is possible to calculate the initial volume of hydrogen present before the liquid was removed from the displacement column, and by recording the volume of hydrogen present at regular intervals the hydrogen production rate and hence the corrosion rate can be obtained.

The gas cell apparatus is shown in Figure 1. The initial state of the cell prior to gas measurement should be:

Rotaflo B - fully open

Rotaflo C - closed

All measurements of liquid height are carried out using a steel ruler calibrated in mm.

A glass vial should be weighed on a balance of the requisite sensitivity (4 decimal points) and then placed under Rotaflo C. A quantity (typically corresponding to 200 to 300 mm in height in the precision bore tube (pbt) of di-n-butyl phthalate (DBP) should be drained and weighed.

The height of DBP in the pbt should be measured before draining (initial height h_1), and 10 minutes after draining (finishing height h_2) to allow time for the DBP to drain from the pbt wall. The atmospheric pressure should be recorded from a digital barometer with a sensitivity of $\pm$0.1 mm/Hg or better. The temperature should also be recorded as the average value of the three equi-spaced thermometers.

Rotaflo B should then be fully closed and the cell removed from the water bath and the height of the DBP reservoir measured (h_{02}).

With reference to Figure 1, the term h_1 corresponds to the DBP level in the precision bore tube (pbt), measured from the top of the side arm perpendicular to the pbt, and h_{01} is the height difference between the same reference point at the base of the pbt and the DBP level in the reservoir before draining. The terms h_2 and h_{02} are the corresponding values after a sample has been removed from the displacement column.

Since the liquid removed comes from both the pbt and the reservoir, the change in the volume of hydrogen in the cell, X, caused by draining off DBP is given by the volume of DBP removed from the column minus the change in the volume of liquid in the displacement column, viz.

$$X = (\text{weight of DBP})/1.047 - (h_1-h_2)\,\pi\, r^2 \quad \text{(A1.1)}$$

where r is the internal radius of the pbt and 1.047 is the density of the DBP in g cm^{-3}.

The value of h_{01} is calculated as follows

$$h_{01} = h_{02} - h \quad \text{(A1.2)}$$

where h is given by

$$h = X/\pi\, r_1^2 \quad \text{(A1.3)}$$

where r_1= radius of the reservoir.

P_1, the hydrogen pressure in the cell (in mm Hg) before draining is

$$P_1 = P_{atmos} + (h_1+h_{01}) \times 1.047/13.6 - WVP \quad \text{(A1.4)}$$

where DBP levels are in mm, 13.6 = density of Hg (g cm^{-3}), 1.047 = density of DBP (g cm^{-3}), WVP = the vapour pressure of water in mm at the test temperature.

P_2, the gas pressure after draining is

$$P_2 = P_{atmos} + (h_2+h_{02})\ 1.047/13.6 - WVP \quad \text{(A1.5)}$$

By definition

$$V_2 = V_1+X \quad \text{(A1.6)}$$

where V_1 and V_2 are the initial and final hydrogen volumes in the cell.

From the ideal gas laws

$$P_1V_1 = P_2V_2 \quad \text{(A1.7)}$$

$$P_1V_1 = P_2(V_1+X) \quad \text{(A1.8)}$$

and

$$V_1 = XP_2/P_1-P_2 \quad \text{(A1.9)}$$

P1, P2 and X are calculated from the measurements of the weight of DBP drained off and the heights of the liquid in the column and in the reservoir (see equations A2.1, A2.2, A2.3, A2.4 and A2.5).

Converting to STP, the initial volume of H_2 in the cell V_0 (in cm^3) is given by

$$V_0 = P_1V_1/T_1\ .\ T_0/P_0 \quad \text{(A1.10)}$$

where T_1 = test temperature in K, T_0 = 273K and P_0 = 760 mm Hg pressure.

When corrosion occurs the associated hydrogen generation causes the DBP level in the pbt to rise. By repeating the above procedure the new volume of hydrogen in the system can be determined, and hence the volume of hydrogen (ΔV) produced by corrosion calculated.

Appendix 2
Corrosion Rate Calculations for Gas Cells

Assuming iron is oxidised in accordance with the following formula

$$Fe + 2H_2O \rightarrow Fe(OH)_2 + H_2 \qquad \text{(A2.1)}$$

this corresponds to 1 mole of oxidised Fe producing 1 mole of H_2.

If the overall corrosion reaction is assumed to be:

$$Fe + 2H_2O \rightarrow Fe(OH)_2 + H_2 \qquad \text{(A2.1)}$$

The reaction corresponds to 1 mole of oxidised Fe producing 1 mole of H_2.

A simple conversion then gives the corrosion in μm.

$$\text{Corrosion} = 10^6 \times (n \times M)/(\rho \times A) \qquad \text{(A2.2)}$$

where

n = no of moles of hydrogen

M = atomic weight Fe (0.05585 kg)

A = surface area (m^2)

ρ = density Fe (7855 kg/m^3)

General conversion factor:

$$1 \text{ mmol } H_2/m^2/yr = 0.0071 \text{ μm/yr} \qquad \text{(A2.3)}$$

For the reaction:

$$3Fe + 4H_2O \rightarrow Fe_3O_4 + H_2 \qquad \text{(A2.4)}$$

the conversion factor is 1 mmol $H_2/m^2/yr$ = 0.0053 μm/yr.

Appendix 3
Refilling the Gas Cell Reservoir

The gas cell apparatus is shown in Figure 1. Prior to removing the gas cell from the water bath Rotaflo B should be fully closed. The following steps were followed:

1. Drain the DBP from the pbt via Rotaflo C. Connect a vacuum hose with in-line valve and a hydrogen line (with a needle valve and a vacuum gauge) to the precision bore tube (pbt) .

2. Close Rotaflo C and evacuate the pbt to -1 bar, close the vacuum valve and open Rotaflo B. Note the majority of the DBP will be drawn up into the pbt.

Close Rotaflo B and drain the DBP via Rotaflo C; clean the pbt by flushing with acetone, and dry glassware with a hot air dryer.

3. Reconnect the vacuum and hydrogen lines and evacuate the pbt to ~-0.2 bar. Close vacuum valve.

4. Connect one end of a rubber hose to Rotaflo C and immerse the other into a beaker of DBP. Slowly open Rotaflo C until liquid has completely filled the nozzle, and then close C.

5. Open the vacuum valve and evacuate to -1.0 bar. Close vacuum valve.

6. Open the needle valve to bring the pressure to 0 bar, then close.

7. Repeat steps (5) and (6) three times, then evacuate to -0.6 bar.

8. Open C and allow DBP to fill the pbt and flask, then close C.

9. Slowly open Rotaflo B to allow DBP to flow into the Dreschel bottle. When the pbt has emptied close B and repeat (8) and (9) until the Dreschel bottle is two thirds full.

10. Slowly open the needle valve and allow the pressure to increase to 0 bar.

11. Close Rotaflo B and remove connection to pbt.

12. Slowly open B to allow DBP to fill the pbt. Tilt the cell to allow air bubbles to escape.

13. Return the cell to the water bath.

ISSN 1404-0344
CM Digitaltryck AB, Bromma, 2005